Journal of the European Ceramic Society **13** (1994) 3–9

Particulate Composites in the Al_2O_3–SiO_2–TiO_2 System by Infiltration Processing

S. J. Li, F. Queyroux & Ph. Boch

Ecole Supérieure Physique Chimie Industrielles, 75231 Paris Cedex 05, France

(Received 13 November 1992; revised version received September 1993; accepted 6 October 1993)

Abstract

Particulate composites in the Al_2O_3–SiO_2–TiO_2 system were prepared by infiltration of pre-sintered alumina skeletons with precursors of silica and titania and subsequent reaction sintering at temperatures $\leq 1600°C$. The microstructure of composites is finer than that of the corresponding 'pure' alumina. It is constituted of alumina grains surrounded by a mullitic, continuous phase.

Einzelne Komposite im System Al_2O_3–SiO_2–TiO_2 wurden durch Infiltration eines vorgesinterten Aluminiumoxid-Skeletts mit Kieselerde- und Titanoxid-Precursorn und anschließendem Reaktionssintern bei Temperaturen $\leq 1600°C$ hergestellt. Das Gefüge der Komposite ist feiner als das des entsprechenden 'reinen' Aluminiumoxids. Es besteht aus Aluminiumoxidkörnern umgeben von einer mullitischen, kontinuierlichen Phase.

Nous avons élaboré des composites à particulaires appartenant au système Al_2O_3–SiO_2–TiO_2 en infiltrant des 'squelettes' d'alumine frittés au préalable avec des précurseurs de silice et d'oxyde de titane, puis en procédant à un frittage réactionnel à des températures $\leq 1600°C$. La microstructure des composites est plus fine que celle de l'alumine 'pure' correspondante. Elle est constituée de grains d'alumine entourés d'une phase mullitique continue.

1 Introduction

Alumina–mullite particulate composites can be prepared by infiltration of pre-sintered, porous alumina skeletons with silica precursors and subsequent reaction sintering,[1–7] using a route which was pioneered by Marple & Green.[1] At the microscopic scale, particulate composites can exhibit better mechanical properties than their constituents, due to reduced grain growth and duplex microstructure, which can lead to higher strength, higher toughness, higher resistance to static fatigue, and better wear and friction properties. At the macroscopic scale, particulate composites can be tailored to yield composition-graded parts. It is possible to develop surface compressive stress, which leads to higher flexural strength due to lower sensitivity to surface cracks and better wear and friction properties due to better control of wear debris. Composition-graded parts allow the surface material to be optimised with respect to certain properties and the core material to be optimised with respect to other properties.

References 1–8 concern binary systems (Al_2O_3–ZrO_2 and Al_2O_3–SiO_2), whereas the present study was devoted to a ternary system (Al_2O_3–SiO_2–TiO_2). Titania was chosen to increase the dielectric properties of mullite–alumina materials, in the framework of a programme on microwave sintering.[9]

2 The Binary Systems Al_2O_3–SiO_2, Al_2O_3–TiO_2 and SiO_2–TiO_2

2.1 The system Al_2O_3–SiO_2

The system Al_2O_3–SiO_2[10] shows a eutectic at $\approx 1590°C$ and a binary compound, mullite. The '3:2' mullite corresponds to $3Al_2O_3$–$2SiO_2$ but there is a solubility domain, ranging from 60 to 66·5 mol% Al_2O_3. Mullite melts congruently or incongruently, depending on experimental conditions. In the equilibrium diagram, the 66·5 mol%–Al_2O_3 mullite melts incongruently at $\approx 1890°C$.

Mullite exhibits excellent high-temperature properties and is widely used in refractory applications. Mullitic materials can be produced by reaction-sintering between alumina and silica:

$$3Al_2O_3 + 2SiO_2 \rightarrow Al_6Si_2O_{13} \text{ (3–2 mullite)}$$

Journal of the European Ceramic Society 0955-2219/94/$7.00 © 1994 Elsevier Science Limited, England. Printed in Great Britain

Mullite is less dense than the starting ($Al_2O_3 + SiO_2$) mixture:

$$(V_{final} - V_{initial})/(V_{initial}) \approx 4\%$$

and, therefore, mullitisation reduces the sintering shrinkage. At the same time, mullite-rich zones within a mullite–alumina composite undergo compressive stress, whereas alumina-rich zones undergo tensile stress. Moreover, mullite exhibits a lower thermal expansion than alumina:

$$\alpha_{20-1000\,C}(Al_6Si_2O_{13}) \approx 5 \times 10^{-6}\,K^{-1}$$

$$\alpha_{20-1000\,C}(Al_2O_3) \approx 9 \times 10^{-6}\,K^{-1}$$

This means that cooling from the sintering temperature leads to compressive stress in mullite-rich zones and tensile stress in alumina-rich zones. As a consequence, a beneficial stress state can be obtained in composition-graded parts with a mullite-rich surface and a mullite-poor core.

2.2 The system Al_2O_3–TiO_2[11,12]

The equilibrium diagram of the system Al_2O_3–TiO_2 shows two eutectics (the lowest one being at $\approx$1705°C) and one binary compound, aluminium titanate (Al_2TiO_5). Aluminium titanate melts congruently at $\approx$1860°C. It is stable from 1860°C to $\approx$1280°C and decomposes below this temperature into $Al_2O_3 + TiO_2$. However, a rapid cooling limits the decomposition of β-Al_2TiO_5 and allows this phase to be kept in a metastable state at room temperature.

β-Al_2TiO_5 single crystals are very anisotropic, which allows polycrystals to exhibit a low average thermal expansion, but with a grain-boundary microcracking. As a consequence, β-Al_2TiO_5 ceramics are very resistant to thermal shocks but they have a low fracture strength.

TiO_2 is sensitive to reduction. For non-perfectly oxidising conditions, TiO_2 can transform into non-stoichiometric TiO_{2-x} and the diagram Al_2O_3–TiO_2 is no longer valid.

2.3 The system SiO_2–TiO_2[13]

This system is the simplest of the three binary systems of interest. There is a eutectic at $\approx$1550°C. The TiO_2 forms no compound with SiO_2. Below $\approx$1550°C, the equilibrium phases are SiO_2 (usually cristobalite) and TiO_2 (usually rutile).

3 The Ternary System Al_2O_3–SiO_2–TiO_2[14,15]

In this diagram (Fig. 1), the dashed straight lines show the compatibility relationships between the solid phases at temperatures of initial melt-formation, the temperatures of B, C, D and E being respectively 1850°C, 1727°C, 1470°C and 1595°C

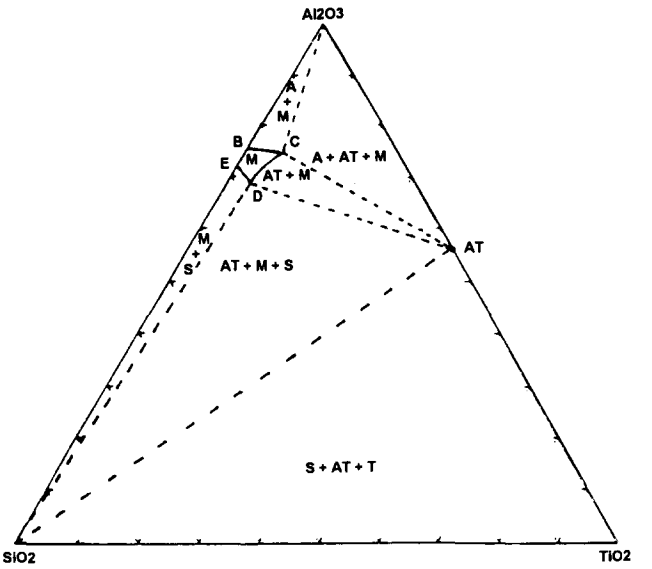

Fig. 1. Phase diagram of the system Al_2O_3–SiO_2–TiO_2 showing solid solution area (adapted from Ref. 19). See the text for symbols.

(A = Al_2O_3, S = SiO_2, T = TiO_2, M = mullite, and AT = aluminium titanate).

- B–C–A α-Al_2O_3 + mullite for $T < 1727$°C
- A–C–AT α-Al_2O_3 + mullite + Al_2TiO_5 for 1280°C < T < 1727°C
- C–D–AT mullite + Al_2TiO_5 for 1280°C < T < 1470°C
- D–AT–S mullite + Al_2TiO_5 + SiO_2 for 1280°C < T < 1470°C
- E–D–S mullite + SiO_2 for 1280°C < T < 1470°C
- S–AT–T $SiO_2 + Al_2TiO_5 + TiO_2$ for 1280°C < T < 1470°C

The temperature of 1280°C corresponds to the eutectic decomposition of Al_2TiO_5. The points B, C, D, and E show the upper limits of the mullite phase with a maximal content of TiO_2 of 4 wt% at C. Mixtures falling within the area BCDE freeze to give mullite only under equilibrium conditions.

For the preparation of particulate composites, the aim was to develop Al_2O_3 as the main phase and mullite as the secondary phase and to limit the residues of other phases—in particular Al_2TiO_5—to low values. This means that the compositions of interest are located inside the triangle A–B–C or close to the line A–C. The composites were heated to a maximum temperature of 1600°C.

4 The Infiltration Processing Technique

The infiltration processing technique requires the pre-sintering of an alumina skeleton to obtain a matrix of a given porosity, then the infiltration by the precursors, and then the reaction-sintering stage.

4.1 Pre-sintering of alumina skeleton

The alumina was a P172SB-Aluminium Péchiney grade, with a composition of 99·70 Al_2O_3, 0·05 Na_2O, 0·05 CaO, 0·08 SiO_2, 0·025 Fe_2O_3 and 0·10 MgO (in wt%) and a mean particle size of $\approx 0{\cdot}65\ \mu m$. The samples were cylindrical pellets, 13 mm in diameter and 7 mm in height, uniaxially pressed under 370 MPa, with no bonding additives. The green density was 60% of theoretical. The open porosity was determined using the Archimedes method, with a de-aerating stage under primary vacuum for 45 min and an immersion in distilled water for 15 min. The pre-sintering treatment was a heating at $2\ ^\circ C\ min^{-1}$ from room temperature to the pre-sintering temperature, a soaking for 3 h, and then a cooling at $5\ ^\circ C\ min^{-1}$. The kiln was an electric one with Super-Kanthal $MoSi_2$ heating elements, working under normal atmosphere. Table 1 gives porosity values versus pre-sintering temperature (the true density of α-Al_2O_3 was taken as $3{\cdot}97\ g\ cm^{-3}$).

The volume of non-alumina phases that can be incorporated into particulate composites depends on the volume of the open porosity of pre-sintered alumina skeletons. The skeletons must not be too fragile to be easily manipulated and, therefore, a compromise must be found between a low temperature of pre-sintering (high porosity but high brittleness) and a high temperature of pre-sintering (low brittleness but low porosity).

Preliminary tests showed that open porosities of about 35% were acceptable and, therefore, the infiltration tests were conducted using 38% porous and 34% porous samples, corresponding to pre-sintering temperatures of 1000°C and 1100°C, respectively. The morphology of open porosity is also a relevant parameter for the infiltration processing. The determination of the pore-size distribution by a mercury intrusion technique showed that the well-dispersed alumina powder that was used as starting material led to pre-sintered parts with a very homogeneous porosity and nearly monosized pores (mean diameter of $0{\cdot}04\ \mu m$ for a pre-sintering temperature of 1000°C).

Table 1. Porosity of pre-sintered Al_2O_3 versus pre-sintering temperature

Pre-sintering temperature (°C)	*Total porosity* (%)	*Open porosity* (%)	*Apparent density* ($g\ cm^{-3}$)
1 000	38	38	2·4
1 075	36	36	2·5
1 100	35	34	2·6
1 150	33	32	2·7
1 200	28	26	2·8
1 300	19	17	3·2
1 400	9	7	3·6
1 500	2	0	3·9

4.2 Infiltrating precursors

The infiltrating precursors must fulfil four main requirements:

(i) The decomposition products must be non-toxic.
(ii) The decomposition temperature must be low, in order not to disturb the final reaction sintering. All the volatile species must be eliminated before the closure of porosity.
(iii) The conversion yield (precursor → ceramic) must be high.
(iv) The viscosity must be low and the surface tension must be high, to facilitate the infiltration.

The infiltration characteristics were studied by Marple & Green[3] who generally used ethyl silicate as the SiO_2 precursor. In the present case of Al_2O_3–SiO_2–TiO_2 materials, various individual precursors for SiO_2 and TiO_2 were studied, such as colloids or solutions. For practical reasons, the use of commercial precursors was preferred. Finally, a good compromise was of using a colloidal silica (high conversion yield and low cost but rather high viscosity)[5] and a soluble titania salt (low conversion yield and high cost but low viscosity).

4.2.1 Silica precursor

The colloidal silica was HS 30 Ludox Dupont de Nemours. The stabilising ion was Na^+, the pH at 25°C was 9·8, the viscosity was 4 Pa. s, and the density was $1{\cdot}21\ g\ cm^{-3}$. The conversion yield to silica was 30 wt%.

4.2.2 Titania precursor

The titania salt was ammonium titanyl oxalate monohydrate ($[NH_4]_2TiO[C_2O_4]_2$–H_2O). Its room temperature solubility was high (1 g of salt for 3 g H_2O). The viscosity of the solution was close to that of water, its density was $1{\cdot}14\ g\ cm^{-3}$, and its conversion yield to titania was 6·6 wt%.

4.3 The infiltration technique

Macroscopically homogeneous materials require a total infiltration of pre-sintered parts whereas composition-graded parts require a partial infiltration only. Besides the characteristics of alumina skeleton and precursor, the other parameters to be taken into account are infiltration sequence, infiltration time, and part thickness. For a given infiltrate and a given part, infiltration depth is controlled by immersion time. Infiltration was carried out at room temperature by immersion of pre-sintered alumina parts into the infiltrate. Drying was done at 110°C for 24 h. Weight measurements were done before infiltration, then after drying and infiltrate decomposition at 900°C. DTA, DTG,

Table 2. Infiltration of Al_2O_3 skeletons with colloidal silica

Pre-sintering temperature (°C)	*Impregnation time* (*h*)	*Weight gain of the part after infiltration and decomposition Experimental/* (*wt%*)	*Filling ratio of pores* (*calculated* (*vol.%*))
1 000	1·5	1·6	28
1 000	2·5	1·7	29
1 000	6	2·3	39
1 000	69·25	4·0	69
1 000	148	5·0	87
1 000	162	5·1	90
1 100	1·5	1·4	30
1 100	2·5	1·5	31
1 100	6	1·9	39
1 100	69·25	3·6	75
1 100	93·25	4·0	88

XRD, and SEM experiments were used to characterise infiltration and subsequent reactions.

4.3.1 Infiltration with colloidal silica

Table 2 gives the data on infiltration, for infiltration times ranging from 1·5 to 162 h.

The weight gain in SiO_2 was higher for the skeletons treated at 1000°C than for those treated at 1100°C but the calculated filling ratio of pores showed an opposite trend. This is because the '1000°C-skeletons' were more porous but the '1100°C-skeletons' had a more favourable ratio between accessible and non-accessible pores. This is due to the fact that the sintering process begins to close the smallest pores, that is, those that were not accessible to the infiltrate. The choice was, therefore, of a pre-sintering temperature of 1000°C for the rest of the study. The standard infiltration time was taken of 148 h, which allows a filling of pores close to 90%.

4.3.2 Infiltration with TiO_2-containing solution

The infiltration with the TiO_2-containing water solution was done on samples previously infiltrated with colloidal silica, then dried at 900°C. Only the residual porosity that was not previously filled with SiO_2 was able to be filled with the TiO_2 solution. Therefore, the residual pores were smaller and more intricate than the initial ones. This was why the TiO_2 precursor had to exhibit a low viscosity to infiltrate the SiO_2-infiltrated parts.

An immersion time of 2 h allowed a filling of pores with the TiO_2 precursor of about 90%. Double and triple infiltrations, with intermediate drying at 900°C, also led to a filling of about 90% of the residual—and decreasing with the number of infiltrations—porosity. This means that particulate composites were able to contain about 5 wt% of SiO_2 and about 0·9, 1·7 and 2·7 wt% of TiO_2 for simple, double, and triple infiltration, respectively. These values correspond to compositions in the triangle A–B–C or close to the line A–C of the ternary diagram, as indicated in Section 3.

5 Reaction Sintering and Microcomposite Development

5.1 Phase evolution

Reaction sintering was conducted according to a thermal cycle similar to that used for the pre-sintering of alumina skeletons, using the same electric furnace. The final soaking temperatures (T) ranged from 1000 to 1600°C, by steps of 50°C. The sample series were labelled as A_{ij}, B_{ij}, C_{ij}, etc., i being the number of infiltrations with the silica precursor (usually $i = 1$) and j the number of infiltrations with the titania precursor (j from 0 to 3).

Experiments were done using four series of samples, with the following compositions:

A_{10} 94·8 wt% Al_2O_3 + 5·2 wt% SiO_2
A_{11} 93·8 wt% Al_2O_3 + 5·1 wt% SiO_2 + 1·1 wt% TiO_2
A_{12} 93·1 wt% Al_2O_3 + 5·1 wt% SiO_2 + 1·8 wt% TiO_2
A_{13} 92·2 wt% Al_2O_3 + 5·0 wt% SiO_2 + 2·8 wt% TiO_2

The results were as in the following sections.

5.1.1 $1000°C \leq T \leq 1100°C$

α-Al_2O_3 was the only phase in A_{10}. α-Al_2O_3 and TiO_2 (rutile) were found in A_{11}, A_{12}, and A_{13}.

The absence of any XRD line relative to quartz or cristobalite showed that silica was still amorphous at the end of treatment.

5.1.2 $T = 1150°C$

α-Al_2O_3 and β-SiO_2 (cristobalite) were found in all samples. TiO_2 (rutile) was found in the TiO_2-containing samples.

5.1.3 $1200°C \leq T \leq 1450°C$

There was a progressive decrease in the β-cristobalite peaks at $T > 1200°C$ for the TiO_2-containing samples (A_{11}, A_{12}, and A_{13}) and $T > 1300°C$ for the TiO_2-free sample (A_{10}). β-cristobalite was not detected in samples treated at 1250°C (A_{11}, A_{12}, and A_{13}) or 1350°C (A_{10}).

The crystallisation of mullite began to be seen at $T \geq 1350°C$ (A_{11}, A_{12}, and A_{13}) or $T \geq 1400°C$ (A_{10}).

The TiO_2 peaks did not exhibit any noticeable changes. However, some traces of Al_2TiO_5 were found in sample A_{13} treated at $T \geq 1400°C$.

These data demonstrate three things:

(i) The presence of titania helps the mullite formation, as indicated by McGee & Wirkus.[16]
(ii) Mullite or mullite-like materials begin to form an amorphous phase before they crystallise.
(iii) The solubility of TiO_2 into mullite-like materials is low at $T < 1450°C$.

5.1.4 $1500°C \leq T \leq 1600°C$

α-Al_2O_3 and mullite were the only crystalline phases in samples A_{10} and A_{11}. α-Al_2O_3, mullite, and Al_2TiO_5 were found in samples A_{12} and A_{13}.

For the highest temperatures (1550°C and 1600°C), there was a decrease in the intensity of the Al_2TiO_5 peaks, which suggested that TiO_2 had entered mullite. Even though it was not possible to determine the exact chemical composition of the mullite formed at 1550–1600°C, the previous assumption is in agreement with literature data that indicate that the maximum solubility of TiO_2 into alumina is about 0·4 wt%,[17] whereas the solubility into mullite goes up to 4 wt%.[15,18] The dissolution of TiO_2 into mullite decreases the amount of titania that can react with alumina to give Al_2TiO_5.

All the XRD data showed some discrepancies between the two faces (superior and inferior) of pellets, which indicated that the infiltrate was redistributed during the post-infiltration treatments, as discussed by Marple & Green.[3] Tests conducted on sawn samples showed that the concentrations of mullite and aluminium titanate were higher at the surface of the pellet than within the core. Such concentration gradients could be exploited to optimise composition-graded parts.

5.2 Sintering shrinkage

A dilatometric study was conducted on four samples, with the following compositions:

B_{10} 94·6 wt% Al_2O_3 + 5·4 wt% SiO_2
B_{11} 93·4 wt% Al_2O_3 + 5·7 wt% SiO_2 + 0·9 wt% TiO_2
B_{12} 92·8 wt% Al_2O_3 + 5·3 wt% SiO_2 + 1·9 wt% TiO_2
B_{13} 92·4 wt% Al_2O_3 + 5·0 wt% SiO_2 + 2·6 wt% TiO_2

The volume shrinkage was defined as:

$$S_{vol}(\%) = [(V_{1000} - V_T)/V_{1000}] \times 100$$

where V_{1000} and V_T were the apparent volume of pellets after firing at 1000°C and T°C, respectively. Figure 2 gives S_{vol} versus T. It shows that the shrinkage rate increases when the TiO_2 content increases, which indicates that titania favours densification, as noticed in Refs 17 and 19. For the B_{11}, B_{12}, and B_{13} samples, the volume shrinkage reaches its maximum at 1400°C, which corresponds to the development of mullitisation. Precise data on true density of particulate composites is required to allow translation of the shrinkage data into porosity data.

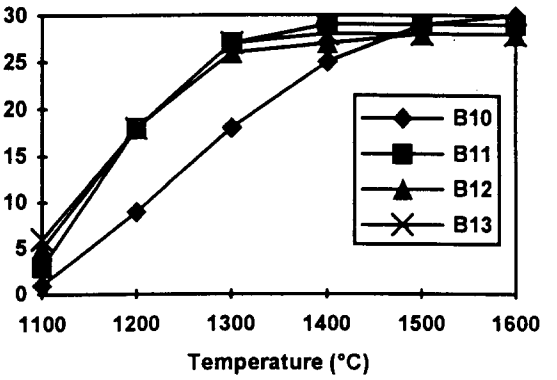

Fig. 2. Volumic shrinkage S_{vol} (in %) versus sintering temperature T (in °C). See the text for symbols.

5.3 Microstructure

A microstructural study was conducted on five samples, with the following compositions:

C_{00} 99·7 wt% Al_2O_3
C_{10} 94·5 wt% Al_2O_3 + 5·5 wt% SiO_2
C_{11} 93·6 wt% Al_2O_3 + 5·3 wt% SiO_2 + 1·1 wt% TiO_2
C_{12} 92·8 wt% Al_2O_3 + 5·4 wt% SiO_2 + 1·8 wt% TiO_2
C_{13} 91·8 wt% Al_2O_3 + 5·4 wt% SiO_2 + 2·8 wt% TiO_2

Figures 3(a) to (e) show micrographs of materials sintered at 1600°C. A microanalysis study showed that the light grey zones are alumina whereas the dark grey zones are mullite or mullite + Al_2TiO_5. The description of particulate composites as being constituted of an alumina matrix containing mullite-based particulates is not adequate. Actually, the composites are constituted of a continuous layer of mullite-based material that surrounds non-connected alumina grains. C_{10} and C_{11} samples contain 23 and 28 vol.% of mullite, respectively.

It must be pointed out that TiO_2, which is sometimes considered as promoting grain growth in alumina,[20] does not bring here such a detrimental influence. Even though the TiO_2-containing samples (C_{11}, C_{12}, and C_{13}) exhibit slightly larger grains than the TiO_2-free sample (C_{10}), all the particulate composites exhibit much finer microstructure than 'pure' alumina (C_{00}), with mean grain size of about 3·5 μm instead of 10·5 μm, respectively. Grain size was measured using a linear intercept technique.[21] This property of mullite-alumina composites to resist grain growth is particularly attractive.

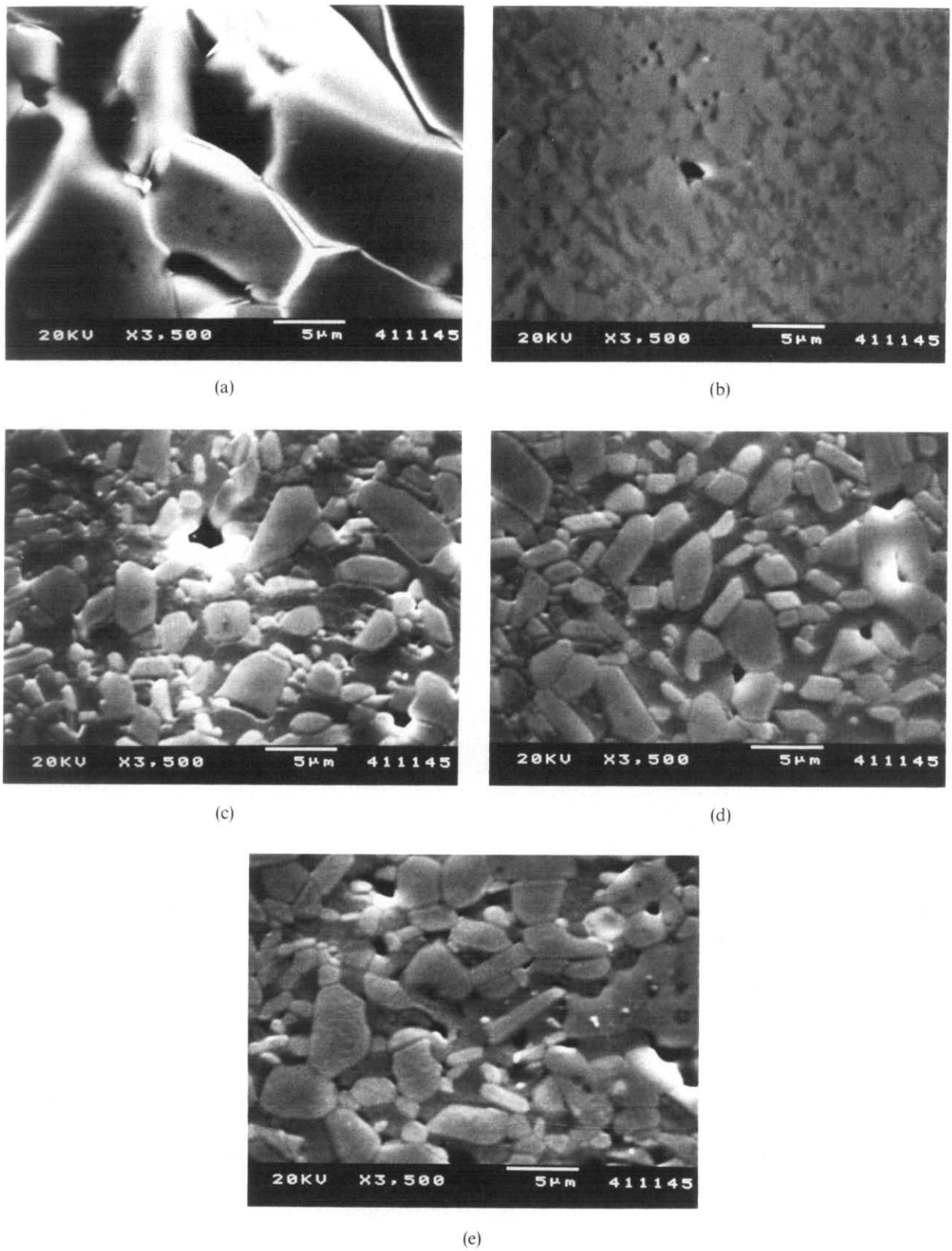

Fig. 3. Micrographs of materials sintered at 1600°C. (a) C_{00}; (b) C_{10}; (c) C_{11}; (d) C_{12}; (e) C_{13}. See the text for symbols.

6 Conclusions

The present study shows that an infiltration processing technique for making ceramic particulate composites can be extrapolated from binary systems to ternary ones. In the case of the system Al_2O_3–SiO_2–TiO_2, it is advantageous to choose a colloid as the SiO_2 precursor and a solution as the TiO_2 precursor. Heat treatments at 1600°C allow all the compositions to be fully reacted and well densified. TiO_2 additions allow a decrease in the maximum temperature of treatment, because they favour both mullitisation and densification. The composites are constituted of alumina grains

surrounded by a mullitic, continuous phase. The mean grain size is finer than that of the corresponding 'pure' alumina.

Acknowledgements

The authors are greatly indebted to F. Lacour for her help in microanalysis and SEM experiments.

References

1. Marple, B. R. & Green, D. J., Incorporation of mullite as a second phase into alumina by an infiltration technique. *J. Am. Ceram. Soc.*, **71**(11) (1988) C471–3.
2. Marple, B. R. & Green, D. J., Mullite/alumina particulate composites by infiltration processing. *J. Am. Ceram. Soc.*, **72**(11) (1989) 2043–8.
3. Marple, B. R. & Green, D. J., Mullite alumina particulate composites by infiltration processing: II, Infiltration and characterization. *J. Am. Ceram. Soc.*, **73**(12) (1990) 3611–16.
4. Root, J. H., Sullivan, J. D. & Marple, B. R., Residual stress in alumina–mullite composites. *J. Am. Ceram. Soc.*, **74**(3) (1991) 579–83.
5. Boch, Ph., Miquel, M. C., Queyroux, F. & Abouaf, M., Mullite–alumina microcomposites. In *Euro-Ceramics 2*, eds G. Ziegler & H. Hausner. Deutsche Keram. Ges. Publ., Köhl, Germany, 1993, pp. 1475–9.
6. Marple, B. R. & Green, D. J., Mullite/alumina particulate composites by infiltration processing: III, Mechanical properties. *J. Am. Ceram. Soc.*, **74**(10) (1991) 2453–9.
7. Marple, B. R. & Green, D. J., Mullite/alumina particulate composites by infiltration processing: IV, Residual stress profiles. *J. Am. Ceram. Soc.*, **75**(1) (1992) 44–51.
8. Glass, S. J. & Green, D. J., Surface modification of ceramics by partial infiltration. *Adv. Ceram. Mat.*, **2**(2) (1987) 129–31.
9. Boch, Ph., Lequeux, N. & Piluso, P., Reaction-sintering of ceramic materials by microwave heating. In *Microwave Processing of Materials III*, Vol. 269, Materials Research Society, Pittsburgh, PA, US, 1992.
10. Klug, F. J., Prochazka, S. & Klug, F. J., Alumina–silica phase diagram in the mullite region. In *Ceramic Transactions*, Vol. 6, *Mullite and Mullite Matrix Composites*, American Ceramic Society, Westerville, OH, US, 1990, pp. 15–45.
11. Kato, E., Daimon, K. & Takahashi, J., Decomposition temperature of β-Al_2TiO_5. *J. Am. Ceram. Soc.*, **63**(5–6) (1980) 355–6.
12. Freudenberg, B. & Mocellin, A., Aluminium titanate formation by solid-state reaction of fine Al_2O_3 and TiO_2 powders. *J. Am. Ceram. Soc.*, **70**(1) (1987) 33–8.
13. de Vries, R. C., Roy, R. & Osborn, E. F., The system titania–silica. *Trans. Brit. Ceram. Soc.*, **53** (1954) 525–40.
14. Agamawi, Y. M. & White, J., The systems Al_2O_3–TiO_2–SiO_2. *Trans. Brit. Ceram. Soc.*, **51** (1952) 293–325.
15. Green, C. R. & White, J., Solid solubility of TiO_2 in mullite in the system Al_2O_3–TiO_2–SiO_2. *Trans. Brit. Ceram. Soc.*, **73**(3) (1974) 73–5.
16. McGee, T. D. & Wirkus, C. D., Mullitization of alumina–silicate gels. *J. Am. Ceram. Soc.*, **51**(37) (1972) 577–81.
17. Bagley, R. D., Cutler, I. D. & Johnson, D. L., Effect of TiO_2 on initial sintering of Al_2O_3. *J. Am. Ceram. Soc.*, **53**(3) (1970) 136–41.
18. Murthy, M. K. & Hummel, F. A., X-Ray study of the solid solution of TiO_2, Fe_2O_3, and Cr_2O_3 in mullite ($3Al_2O_3 . 2SiO_2$). *J. Am. Ceram. Soc.*, **43**(5) (1960) 267–73.
19. Baudin, C. & Moya, J. S., Influence of titanium dioxide on the sintering and microstructure evolution of mullite. *J. Am. Ceram. Soc.*, **67**(7) (1984) C134–6.
20. Gitzen, W. H., *Alumina as a Ceramic Material*. American Ceramic Society, Columbus, OH, US, 1970.
21. Wurst, J. C. & Nelson, J. A., Linear intercept technique for measuring grain size in two-phase polycrystalline ceramics. *J. Am. Ceram. Soc.*, **55**(2) (1972) 109.